Orbital spaces and density-functional theory

C. Gutlé[1] and A. Savin[2]
[1]*Laboratoire Interuniversitaire des Systèmes Atmosphériques, CNRS UMR 7583 et Universités Paris 7 et Paris 12, 94010 Créteil, France*
[2]*Laboratoire de Chimie Théorique, CNRS UMR 7616 et Université Pierre et Marie Curie, 75252 Paris, France*
(Received 1 September 2005; revised manuscript received 14 January 2007; published 26 March 2007)

Only part of the correlation energy can be obtained from the wave function when expanded as a finite and linear combination of Slater determinants. For the remaining part, it was proposed by several authors to use density-functional theory. Thus, various methods coupling wave functions with density functionals were investigated in the past. In the present a class of such methods was developed, relying on a partition of the orbital space. Notably, for this coupled method special efforts were made to avoid double countings between the contributions of the wave function and the density functional. Moreover, the coupling was defined in order to allow a systematic improvement of the results. As a second step, the method was put to the test for spherically symmetric systems, especially in the case of near degeneracy. The numerical results obtained were discussed in order to improve the model. Finally, the wave function contribution that was retained relied on a coupled-cluster formalism restricted to a small orbital space, whereas the density functional was chosen as a semilocal expression based on the physical picture of one-particle ionization potentials.

DOI: 10.1103/PhysRevA.75.032519 PACS number(s): 31.25.Eb, 31.15.Dv, 31.15.Ew

I. INTRODUCTION

After the principles of quantum mechanics were stated and the Schrödinger equation published, the wave function was considered as the relevant quantity giving access to all chemical properties. In particular and quite importantly, the ground-state energy was obtained as the eigenvalue of the Hamiltonian associated with the ground-state wave function. Based on these first principles analytical calculations were early performed on small systems (e.g., atom He, molecule H_2), yielding quite encouraging results at relatively low cost. As a natural continuation practical roads were gradually built in order to connect the crudest starting models to the exact theoretical results. Namely, by adding more Slater determinants in the expansion of the wave function and increasing the orbital space, a path was provided to refine the models systematically (e.g., configurations interactions, many-body perturbation theory, coupled clusters, etc.). Unfortunately, however, it was realized at the same time that further gain in accuracy is payed for by an exponential increase of computational cost. For that reason, it might have been thought that chemical accuracy would remain out of reach. Within that context, two major events reversed this tendency. On the one hand, the field of computer techniques underwent a tremendous growth with respect to storage capacity and processor speed. On the other hand, modern algorithms were developed. As a result, systems of moderate size can be nowadays calculated accurately [1,2].

In parallel with the development of approaches based on the ground-state wave function, it was proposed to extract the ground-state energy from an observable: the ground-state electronic density. Indeed, from this alternative formulation of the theory substantial improvement was expected in the scaling of the associated practical methods. However, at the beginning the approach based on the density was hardly followed as the first approximation proposed by Thomas [3] and Fermi [4] was not able to account for such important physics as chemical bonding. Things changed drastically only with the release of the Kohn-Sham scheme [5], which allowed great progress toward chemical accuracy, so much that, today, density functionals based on that scheme are competing with wave-function-based correlated methods, especially as far as large systems are concerned. Nevertheless, present density functionals still suffer from a serious drawback: no road is known to go from a given density functional to the universal functional that the Hohenberg-Kohn theorem [6] proved to exist.

The current work can be viewed as a continuation of [7,8]. The purpose is twofold. First, to try to retain the best of the two above-mentioned worlds: the systematic improvement property of the wave function approach and the favorable scaling of the density functional methods. Second, to get rid of their respective drawbacks: the slow convergence of the wave function representation and the uncontrolled errors of density functionals. In that goal a coupled method based on both the wave function and the density will be defined. Then, the main challenge will be to guarantee as much as possible the complementarity of each method within the coupling. As a first step, in this work focus will be put on the calculation of the ground-state energy.

The approach exposed in this paper can be viewed as a variant of the two Kohn-Sham schemes [5]. A discussion of this topic is available from EPAPS (Sec. I) [9]. Indeed, whereas the Kohn-Sham schemes rely on exchange-correlation and correlation density functionals, respectively, in the present only part of the correlation energy is required to be handeled by a density functional, the complement being provided by a wave function. In order to fix the separation between the two components of the correlation energy in a practically efficient way, we resort to an analysis in terms of the wave function (Sec. II). In particular, within that context the delicate situation of atomic near degeneracies is addressed. To start with the analysis, we note the arbitrariness in the definition of the correlation energy. This point is argumented in the EPAPS material (Sec. II) [9]. Consequently, it is decided to retain in the following the definition of the correlation energy leading to the most tractable approxima-

tions. In that respect, we examine the suitability of the methods based either on the wave function or on the density (Sec. II A). The arguments all boil down to the assumption that a convenient strategy would be to build a coupled method involving both the wave function and the density, where the near degeneracies are devoted to the wave function and the remaining to the density (Sec. II B). After these preliminaries the principle of the solutions investigated is detailed (Sec. III) and the starting approximations defined (Sec. V). In Sec. VI, further refinements of these approximations are motivated by numerical tests. The results presented deal with the first ten terms of each cationic isoelectronic series: He, Be, Ne, Mg, and Ar. By that choice it is intended to probe the present approach both in the presence and in the absence of angular near degeneracies. As a conclusion (Sec. VII), the method is revealed to be accurate and moderate in cost at the same time for these systems. Therefore it is suggested that in future work calculations be performed within the same scheme and, for more general systems like molecules, at the equilibrum as well as dissociating geometry.

II. PARTITIONING THE CORRELATION ENERGY

Our purpose in this section is to justify our partitioning of the correlation energy into two components. Following from this a specific division is proposed, based on the orbital space (Sec. II A). Finally the resulting two components are attributed to either a wave function or a density-functional treatment (Sec. II B).

A. Two scales for the correlation energy

Let us assume that the wave function has been expanded as a linear combination of Slater determinants. In quantum chemistry, part of this wave function, including one or a few determinants, is usually chosen as the reference wave function. In order to give a simple picture, the resulting correlation energy E_c is then produced by exciting that reference wave function in the complementary virtual orbital space. Three contributions can be isolated:

$$E_c = E_c^l + E_c^h + E_c^{lh}. \tag{1}$$

The first arises from excitations in the low-energy part of the one-particle spectrum (E_c^l), the second from the high-energy excitations (E_c^h), and the third from mixed low- and high-energy excitations (E_c^{lh}). As an illustration, one possible diexcitation of a single-determinant reference wave function is represented in Fig. 1.

Among the above three components two are quite distincts. On the one hand, E_c^l accounts for effects that are specific to the system. These effects are often directly related to the gap between the highest occupied molecular orbitals (HOMO's) and the lowest unoccupied molecular orbitals (LUMO's): accidental or nonaccidental degeneracies, near degeneracies. By contrast, in E_c^h the virtual orbitals ressemble much more each other, and therefore their contribution is often considered as less specific.

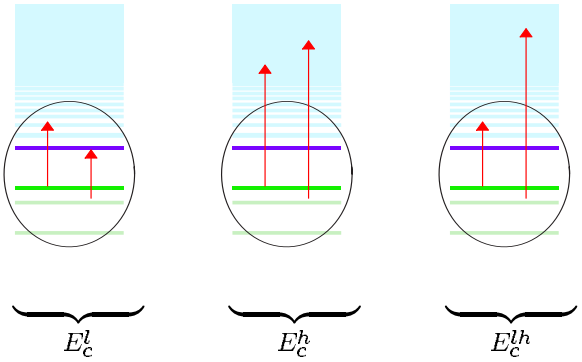

FIG. 1. (Color online) Low-energy diexcitations E_c^l (left), high-energy diexcitations E_c^h (middle), mixed low- and high-energy diexcitations E_c^{lh} (right)

B. Strategy: One method for each energy scale

From a practical point of view the following problem is encountered when dealing with E_c as written in Eq. (1). Of course, formalisms based on the wave function allow accurate calculations of the low-energy component E_c^l, which is described within a restricted orbital subspace. By contrast, the remaining part $E_c^h+E_c^{lh}$, obtained by summing an infinite number of terms, is always prohibitive. Alternatively formalisms based on the density lead exactly to the opposite conclusions, as will be seen later on: even though a reasonable estimation for the high-energy component E_c^h can usually be obtained, this time this is the low-energy part of the calculation which is often found into be great error. Briefly, none of the two approaches based on either the wave function or the density seems to be suited for calculating all the components of E_c. To solve this dilemma it is suggested here to develop a coupled method where E_c^l is evaluated from a wave function and E_c^h from a density functional. For the mixed term E_c^{lh}, where the error is expected to be smaller, either a density functional or a wave function will be used (this point will be discussed in Sec. III B). These prescriptions are summerized in Eq. (2):

$$E_c = \underbrace{E_c^l}_{accurate} + \underbrace{E_c^h}_{approx} + \underbrace{E_c^{hl}}_{accurate\ or\ approx}. \tag{2}$$

In that formula separation still has to be specified between low- and high-energy excitations. For our purpose, which is the proper description of all the components in E_c, the optimal separation will be the one allowing the better efficiency for both E_c^l and E_c^h. As that optimal separation is expected to depend on the system under investigation, it is decided, at a preliminary stage, to control it by a parameter acting on the virtual space. However, we hope the quality of the results is stable in an interval of parameters, so that, ultimately, the choice of the parameter is not decisive within that interval. Two separations will be described in next section, together with their associated parameters.

III. PRINCIPLE OF THE METHOD

The principle of the method proceeds from three steps. First, a fictitious system is defined, depending on a parameter

p. The corresponding Hamiltonian is quoted as $\hat{H}^p$ and its correlation energy E_c^p. Second, the correlation energy of the real system, E_c, is expressed from the one of the fictitious system, E_c^p, according to

$$E_c = E_c^p + \Delta E_c^p. \tag{3}$$

Thus, in Eq. (3), ΔE_c^p is defined as the difference between E_c and E_c^p. Third, each of the two components E_c^p and ΔE_c^p is assigned to an approach, based on Ψ or ρ, with two options: either E_c^p is evaluated with a wave function (we then note $E_c^p = E_{cw}$) and ΔE_c^p with a density functional (we then note $\Delta E_c^p = E_{cd}$) or, conversly ($E_c^p = E_{cd}$ and $\Delta E_c^p = E_{cw}$).

Let us go to the first step. Two different fictitious systems will be defined as attempts to make a proper separation between E_{cw} and E_{cd}, as mentioned in the strategy of Sec. II B. For the first one, the virtual one-particle levels will be shifted by a positive constant, whereas for the second the highest virtual one-particle levels will be truncated. The results of the couplings based on these two fictitious systems will be compared.

A. Fictitious systems with gap shift and with cutoff

The Hamiltonian $\hat{H}^G$ of the fictitious system with a gap shift G depends upon the coupling parameter G as follows:

$$\hat{H}^G = \hat{T} + \hat{V}^G + \hat{V}_{ee} + \hat{P}^G, \tag{4}$$

where $\hat{T}$ and $\hat{V}_{ee}$ are the kinetic and Coulomb operators, respectively, $\hat{V}^G$ is an arbitrary local potential depending on paraneter G, and $\hat{P}^G$ obeys

$$\hat{P}^G = G\sum_{n=1}^{N}\sum_{i} |D_{n_i}\rangle\langle D_{n_i}|. \tag{5}$$

In the above equation D_{n_i} is the ith n excited determinant, with respect to the arbitrary reference determinant D_0. For instance, if D_0 is the Kohn-Sham determinant, the D_{n_i}'s are obtained by substituting n occupied with n virtual Kohn-Sham (KS) orbitals. The system with gap shift can be solved by following either the wave function or the density approach. In the latter case, note that the Hohenberg-Kohn theorem [6] holds. Namely, if $\hat{V}^G$ can be made such that the density of the fictitious system with Hamiltonian $\hat{H}^G$ equals the density of the true system, then $\hat{V}^G$ is uniquely defined by this prescription. Hence the system with gap shift can be described by a universal functional of both the density and parameter G. Now, two limit situations are distinguished for $\hat{P}^G$ according to the value of G. For $G=0$, $\hat{H}^G$ is identical to the Hamiltonian of the true system—that is to say, the fully interacting system (FIS). For $G\to\infty$, all determinants D_{n_i} except the reference D_0 have their energy translated to infinity. Consequently, Hamiltonian $\hat{H}^{G\to\infty}$ refers to a noninteracting system, either KS or Krieger-Li-Iafrate (KLI) depending on our choice for generating the orbitals in projector $\hat{P}^G$. Let us mention, eventually, that the correlation energy in the system with gap shift, E_c^G, is a continuous function of G in the interval $G \in [0,\infty[$.

The second fictitious system studied will be referred to as the system with cutoff κ, where κ is a chosen parameter. It is defined so that the virtual orbitals with energies greater than κ do not interact with the occupied orbitals in the expansion of the N-particle wave function as a linear combination of Slater determinants. Such a system can be obtained, for instance, by shifting the virtual orbitals with energies greater than κ to sufficiently high energy.[1] The Hamiltonian $\hat{H}^\kappa$ of the system with cutoff is thus written as

$$\hat{H}^\kappa = \hat{T} + \hat{V}^\kappa + \hat{V}_{ee} + \hat{P}^\kappa, \tag{6}$$

where $\hat{V}^\kappa$ is an arbitrary local potential and $\hat{P}^\kappa$ the projector:

$$\hat{P}^\kappa = \sum_{n=1}^{N}\sum_{i}\prod_{j=1}^{N}\theta_{\kappa-\epsilon_{n_i j}}|D_{n_i}\rangle\langle D_{n_i}|. \tag{7}$$

θ is a step function (θ_x is large if $x>0$; it is zero otherwise). In Eq. (7), orbitals energies $\epsilon_{n_i j}$ are labeled with a double index. The i index refers to the determinant the orbital belongs to, and j indicates the position of the orbital within the determinant. Thus, with that convention a given orbital energy is quoted as $\epsilon_{n_i j}$ when attached to D_{n_i} and as $\epsilon_{n_{i'} j'}$ when attached to $D_{n'_i}$, j being possibly different from j'. From Eqs. (6) and (7) it follows that Hamiltonian $\hat{H}^\kappa$ gives high energies to a class of determinants D_{n_i}, which then contribute weakly to the wave function. Those D_{n_i} determinants are made of at least one orbital having energy $\epsilon_{n_i j}$ ($j \in [1,N]$) above parameter κ. As in the gap shift variant discussed above, if $\hat{V}^\kappa$ can be built in such a way that the density of the fictitious system of Hamiltonian $\hat{H}^\kappa$ is equal to the density of the true system, it is uniquely defined. The two limits of $\hat{H}^\kappa$ are as follows. When $\kappa\to\infty$, all D_{n_i}'s are selected by the projector and $\hat{H}^{\kappa\to\infty}$ corresponds to the Hamiltonian of the FIS. On the contrary, when κ equals the energy of the highest occupied orbital in the reference determinant, ϵ_{homo}, only this reference determinant is selected by the projector, as in a noninteracting system (NIS). Contrary to the situation with gap shift previously envisioned, for the system with a cutoff E_c^κ is a discontinuous function of the parameter κ in the interval $\kappa \in [\epsilon_{homo},\infty[$.

B. Energy scales and couplings

The partitioning of the correlation energy described in Sec. II A and schematized in Fig. 1 for the fully interacting system can be extended to the fictitious systems defined in Sec. III A. As far as the system with a gap shift is concerned, E_c^G can be viewed as resulting from excitations in a one-particle spectrum where the virtual orbitals have been shifted in energy by G (Fig. 2, left). Therefore, for sufficiently large

[1] There are difficulties using the Hohenberg-Kohn theorem in finite space (one of them is mentionned in [31]). This problem shows up with the cutoff operator. However, they can be avoided by not totally eliminating the virtual states beyond κ, but by keeping them with a negligible weight.

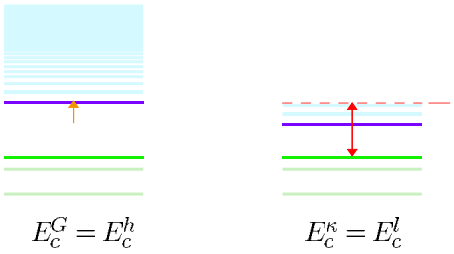

FIG. 2. (Color online) One-particle spectrum associated with the fictitious systems with gap shift G (left) and cutoff κ (right).

G one might expect the correlation energy of the system with gap shift to result mainly from high-energy excitations in the shifted spectrum—i.e., $E_c^G \approx E_c^h$. Alternatively, for the fictitious system with cutoff the correlation energy is obtained from excitations in a one-particle spectrum where orbitals with energies greater than κ have been removed (Fig. 2, right). Thus, in that case the truncated correlation energy is expected to contain low-energy excitations only—i.e., $E_c^\kappa = E_c^l$.

Collecting the results for the fictitious systems allows us to go one step further and analyze the correlation energy of the fully interacting system (3) within the context of the coupled methods proposed in this paper. Thus, in the gap shift variant $E_c^G = E_c^h$ and $E_c - E_c^G = E_c^l + E_c^{lh}$ (Fig. 3) whereas in the cutoff variant $E_c^\kappa = E_c^l$ and $E_c - E_c^\kappa = E_c^h + E_c^{lh}$ (Fig. 4). According to the introduction of Sec. III, identification of the components E_c^l, E_c^h, and E_c^{lh} of the correlation energy with the quantities E_c^p and ΔE_c^p [Eq. (3)] closes step 2 for defining the present couplings. The third step will be discussed in the next section.

C. One method for each energy scale within the couplings

According to Sec. III A the methods based on Ψ (ρ) are expected to be especially suited for describing the correlation arising from the low- (high-) lying states E_c^l (E_c^h). Moreover, in Sec. III B, ΔE_c^h and ΔE_c^h have been related to the low and high regions of the one-particle spectrum in the gap shift and cutoff variants. From these arguments it is expected that the following assignments reveal a more efficient approach. For

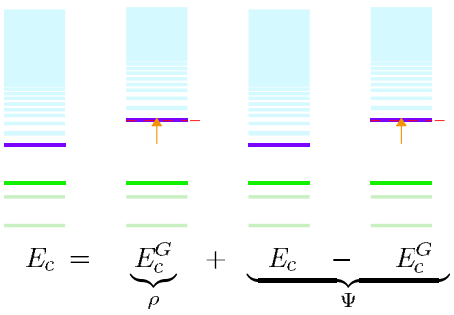

FIG. 3. (Color online) One-particle spectra for the exact coupling with gap shift. From left to right: FIS, partially interacting system with gap shift, FIS, and partially interacting system with gap shift. Ψ (ρ) designates the part of the calculation deferred to the wave function (density) approach.

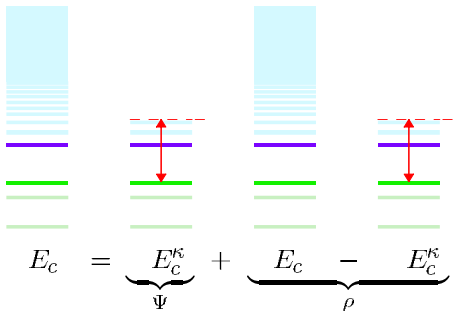

FIG. 4. (Color online) One-particle spectra for the exact coupling with cutoff. From left to right: FIS, partially interacting system with cutoff, FIS, and partially interacting system with cutoff. Ψ (ρ) designates the part of the calculation deferred to the wave function (density) approach.

the gap shift variant of the coupling the high excitation energies are given by $E_{cd} = E_c^G$—i.e., through a density functional scheme—and the residue by $E_{cw} = E_c - E_c^G$—i.e., through a wave function scheme. We remind the reader that the notation E_{cw} (E_{cd}) means that the corresponding component of the correlation energy is evaluated with a wave-function- (density-functional-) based approach. For the cutoff variant, by contrast the low-energy excitations should be given by $E_{cw} = E_c^\kappa$ and the residue by $E_{cd} = E_c - E_c^\kappa$. By completion of this third step, the couplings with gap shift and cutoff have now been defined.

IV. THEORY

In the preceding sections the principle of the couplings has been presented. Here we complement this point by giving the corresponding equations that have been used. The ground-state energy a system with Hamiltonian

$$\hat{H}_V = \hat{T} + \hat{V}_{ee} + \hat{V} \tag{8}$$

is

$$E_{0,v} = \min_\rho \left\{ F[\rho] + \int v\rho \right\}, \tag{9}$$

where $\hat{V} = \Sigma_{i=1}^N v(i)$ is an arbitrary potential and $F[\rho]$ is a universal functional of the density in the sense that it does not depend on potential v. Following Levy [10], $F[\rho]$ is written as

$$F[\rho] = \min_{\Psi \to \rho} \langle \Psi | \hat{H}_V - \hat{V} | \Psi \rangle = \min_{\Psi \to \rho} \langle \Psi | \hat{T} + \hat{V}_{ee} | \Psi \rangle = T[\rho] + V_{ee}[\rho]. \tag{10}$$

In this formula $T[\rho] = \langle \Psi_\rho | \hat{T} | \Psi_\rho \rangle$ and $V_{ee}[\rho] = \langle \Psi_\rho | \hat{V}_{ee} | \Psi_\rho \rangle$, where Ψ_ρ is the wave function with density ρ, which minimizes $\langle \hat{T} + \hat{V}_{ee} \rangle$. $F[\rho]$ can also be expressed as

$$F[\rho] = \langle \Psi^{KS} | \hat{H}_V - \hat{V} | \Psi^{KS} \rangle + E_c[\rho] = T_s[\rho] + J[\rho] - K[\rho] + E_c[\rho], \tag{11}$$

where Ψ^{KS} is the Kohn-Sham wave function associated with

the system defined in Eq. (8), $T_s[\rho]$ and $J[\rho]$ the kinetic and Coulomb functionals built on Ψ^{KS}, and $K[\rho]$ the exchange functional defined as $J[\rho]-\langle\Psi^{KS}|\hat{V}_{ee}|\Psi^{KS}\rangle$. $E_c[\rho]$ is defined by Eq. (11). The same derivations can be repeated for the fictitious system with Hamiltonian

$$\hat{H}^p_{V^p} = \hat{T} + \hat{V}^p{}_{ee} + \hat{O}^p + \hat{V}^p, \tag{12}$$

where $\hat{O}^p$ is a projector operator acting on the virtual Kohn-Sham orbitals. The Hamiltonians for the fictitious systems with gap shift and cutoff [defined in Eqs. (4) and (6), respectively] have clearly this form. The universal functional of the density related to $\hat{H}^p_{V^p}$ as defined by Eq. (12) is

$$F^p[\rho] = \min_{\Psi\to\rho}\langle\Psi|\hat{H}^p_{V^p} - \hat{V}^p|\Psi\rangle = \min_{\Psi\to\rho}\langle\Psi|\hat{T} + \hat{V}_{ee} + \hat{O}^p|\Psi\rangle$$
$$= \langle\Psi^p_\rho|\hat{T} + \hat{V}_{ee} + \hat{O}^p|\Psi^p_\rho\rangle, \tag{13}$$

where Ψ^p_ρ is the wave function with density ρ, which minimizes $\langle\hat{T}+\hat{V}_{ee}+\hat{O}^p\rangle$. The expression involving the Kohn-Sham orbitals is

$$F^p[\rho] = \langle\Psi^{KS}|\hat{H}^p_{V^p} - \hat{V}^p|\Psi^{KS}\rangle + E_c[\rho] = T_s[\rho] + J[\rho] - K[\rho]$$
$$+ E^p_c[\rho], \tag{14}$$

as matrix element $\langle\Psi^{KS}|\hat{O}^p|\Psi^{KS}\rangle$ which comes out in the development of $\langle\Psi^{KS}|\hat{H}^p_{Vp}|\Psi^{KS}\rangle$ is zero (projection operator $\hat{O}^p$ only acts on virtual Kohn-Sham orbitals by definition). At this stage $F[\rho]$ can be expressed through the identity $F[\rho] = F[\rho]+F^p[\rho]-F^p[\rho]$. Then, by replacing $F[\rho]$ and $F^p[\rho]$ with the right-hand sides of Eqs. (11) and (14), respectively, we obtain

$$F[\rho] = T_s[\rho] + J[\rho] - K[\rho] + E^p_c[\rho] + E_c[\rho] - E^p_c[\rho]. \tag{15}$$

The terms on the right-hand side of Eq. (15) can be grouped in two different ways. Either the last term $E^p_c[\rho]$ is treated with a density functional and the others with a wave function or the last two terms $E_c[\rho]-E^p_c[\rho]$ are treated with a density functional and the other with a wave function. The former case corresponds to the coupling with gap shift and the latter to the coupling with cutoff, in agreement with the arguments of Sec. III.

V. STARTING APPROXIMATIONS

After the theoretical grounds of the couplings have been settled, some approximations are needed in order to produce numerical results. In this section they are introduced and put to the test for the cationic isoelectronic series of He, Be, Ne, Mg, and Ar. Indeed these systems are sufficiently simple to allow accurate calculations to validate the method numerically. Moreover, they are at the same time sufficiently complex to show sensitive correlation effects such as angular near degeneracies. Finally, the correct description of the correlation energy in those systems still remains a challenge for present approximate density functionals [11–13].

A. Inequalities for the ground-state energy

According to Eq. (9) the ground-state energy of the system with external potential $\hat{V}_{ne}$ can be expressed as $E_{0,v_{ne}} = \min_\rho\{F^p[\rho]+\bar{F}^p[\rho]+\int\rho v_{ne}\}$ where $\bar{F}^p[\rho]=F[\rho]-F^p[\rho]$. We further develop that expression by replacing $F[\rho]$ with its definition in Eq. (10):

$$E_{0,v_{ne}} = \min_\rho\left\{\min_{\Psi\to\rho}\langle\Psi|\hat{H}^p_V - \hat{V}|\Psi\rangle + \bar{F}^p[\rho] + \int\rho v_{ne}\right\} \tag{16}$$

$$= \min_\rho\left\{\min_{\Psi\to\rho}\langle\Psi|\hat{H}^p_V|\Psi\rangle + \bar{F}^p[\rho] + \int\rho(v_{ne}-v)\right\} \tag{17}$$

$$= \langle\Psi^p_{\rho_0}|\hat{H}^p_V|\Psi^p_{\rho_0}\rangle + \bar{F}^p[\rho_0] + \int\rho(v_{ne}-v), \tag{18}$$

where ρ_0 is the ground-state density of $\hat{H}_V$ and $\Psi^p_{\rho_0}$ is the wave function with density ρ_0, which minimizes $\hat{H}^p_V$. Different choices can be made for V in the above equations. In particular, $V=V^p$ allows the fictitious system with Hamiltonian $\hat{H}^p_{Vp}$ to reproduce the density of the true system whatever p, as mentioned in Sec. III A. Alternatively, for practical convenience we will choose V to equal the nucleus-electron potential V_{ne}, independent of p. In that case, Eq. (18) becomes $E_{0,v_{ne}} = \langle\Psi^p_{\rho_0}|\hat{H}^p_{V_{ne}}|\Psi^p_{\rho_0}\rangle + \bar{F}^p[\rho_0]$. In that case, however, $\Psi^p_{\rho_0}$ is not the ground state of $\hat{H}^p_{V_{ne}}$ (which is Ψ^p), and hence the wave function and density parts of the coupling have to be evaluated self-consistently. To avoid that, the following inequalities can be written by following Refs. [14–16]:

$$\langle\Psi^p|\hat{H}^p_{V_{ne}}|\Psi^p\rangle + \bar{F}^p[\rho_0] \leqslant E_{0,v_{ne}} \leqslant \langle\Psi^p|\hat{H}^p_{V_{ne}}|\Psi^p\rangle + \bar{F}^p[\rho[\Psi^p]], \tag{19}$$

where $\rho[\Psi^p]$ is the density yielded by Ψ^p. Moreover, in these inequalities we will only calculate the right-hand side as an upper-bound approximation to $E_{0,v_{ne}}$. Indeed, we presently expect the error in our ansatz for the density functional to be larger than the one induced by inputting an approximate density in it. As a consequence, we assume $\bar{F}^p[\rho_0] \approx \bar{F}^p[\rho[\Psi^p]]$.

B. Replacing the Kohn-Sham wave function with another reference wave function

The two terms on the right-hand side of Eq. (19) can be transformed as follows. For $\langle\Psi^p|\hat{H}^p_{V_{ne}}|\Psi^p\rangle$ we add and substract $\hat{V}_{ne}$, and introduce the functional $F^p[\rho[\Psi^p]]$ as defined in Eq. (13):

$$\langle \Psi^p | \hat{H}^p_{V_{ne}} | \Psi^p \rangle = \langle \Psi^p | \hat{H}^p_{V_{ne}} - \hat{V}_{ne} | \Psi^p \rangle + \int \rho[\Psi^p] v_{ne}$$

$$= F^p[\rho[\Psi^p]] + \int \rho[\Psi^p] v_{ne}. \quad (20)$$

We notice that $F^p[\rho[\Psi^p]]$ can also be evaluated by using a reference wave function Ψ^{ref} other than Kohn-Sham through

$$F^p[\rho[\Psi^p]] = \langle \Psi^{ref} | \hat{H}^p_{v_{ne}} - \hat{V}_{ne} | \Psi^{ref} \rangle + E^p_c[\rho[\Psi^p]]. \quad (21)$$

In that way, the correlation energy $E^p_c[\rho[\Psi^p]]$ is no longer defined with respect to Ψ^{KS}, as in Eq. (14). It is now defined with respect to Ψ^{ref}. The only requirement for equality (21) to hold is that Ψ^{ref} is a functional of the density. Such is the case, in particular, for Hartree-Fock and Krieger-Li-Iafate wave functions [17], as they are uniquely defined by the Hamiltonian. By inputing Eq. (21) into Eq. (20) and grouping the terms involving v_{ne} we obtain

$$\langle \Psi^p | \hat{H}^p_{V_{ne}} | \Psi^p \rangle = \langle \Psi^{ref} | \hat{H}^p_{v_{ne}} | \Psi^{ref} \rangle + E^p_c[\rho[\Psi^p]] + \int (\rho[\Psi^p]$$

$$- \rho[\Psi^{ref}]) v_{ne}. \quad (22)$$

The reference wave function can also be placed in the second term in Eq. (19). Indeed, as for $F^p[\rho[\Psi^p]]$ in Eq. (21) we find $F[\rho[\Psi^p]] = \langle \Psi^{ref} | \hat{H}_{v_{ne}} - \hat{V}_{ne} | \Psi^{ref} \rangle + E_c[\rho[\Psi^p]]$. Following from that we obtain

$$\bar{F}^p[\rho[\Psi^p]] = F[\rho[\Psi^p]] - F^p[\rho[\Psi^p]] = E_c[\rho[\Psi^p]]$$

$$- E^p_c[\rho[\Psi^p]]. \quad (23)$$

Eventually, by replacing each term on the right-hand side of Eq. (19) according to Eqs. (20) and (23), we obtain

$$E_{0,v_{ne}} \leqslant \langle \Psi^{ref} | \hat{H}^p_{v_{ne}} | \Psi^{ref} \rangle + \int (\rho[\Psi^p] - \rho[\Psi^{ref}]) v_{ne}$$

$$+ E^p_c[\rho[\Psi^p]] + E_c[\rho[\Psi^p]] - E^p_c[\rho[\Psi^p]]. \quad (24)$$

In the above expression, the last two terms will be treated with a density functional and the others with a wave function. That scheme corresponds, in particular, to the cutoff variant of the couplings. We perform the following approximations: for the wave function part, $\int (\rho[\Psi^p] - \rho[\Psi^{ref}]) v_{ne}$ is neglected and for the density part we use $\rho[\Psi^{ref}]$ in replacement of $\rho[\Psi^p]$. The argument is the same as in last subsection; we do not expect the discrepancy in the density to be the major source of errors in our calculations, given our ansatz for the density functional. An inequality similar to (24) is obtained if emphasis is put on F^p instead of $\bar{F}^p$:

$$E_{0,v_{ne}} \leqslant \langle \Psi^{ref} | \hat{H}^p_{v_{ne}} | \Psi^{ref} \rangle + \int (\rho_0 - \rho[\Psi^{ref}]) v_{ne} + E_c[\rho_0]$$

$$- E^p_c[\rho[\Psi^p]] + E^p_c[\rho[\Psi^p]]. \quad (25)$$

In that case, a density functional will be used for the last term and a wave function for the others. The approximations are the same as previously ($\int (\rho[\Psi^p] - \rho[\Psi^{ref}]) v_{ne} \approx 0$ and $\rho[\Psi^p] \approx \rho[\Psi^{ref}]$) for the same reason (see Ref. [15] for more justifications for that approximation). That scheme corresponds, in particular, to the gap shift variant of the couplings.

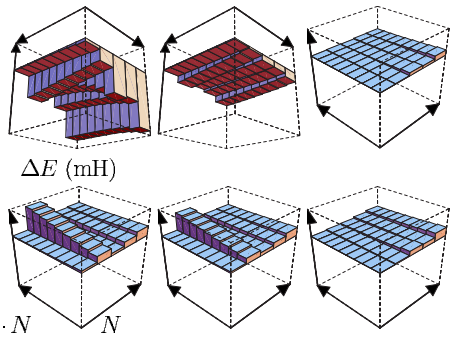

FIG. 5. (Color online) On the vertical axis, error ΔE of a given method in mhartree (from −100 to +50). On the left axis, charge of the system $Z-N$ (from 0 to 8); on the right axis, number of electrons, N, (2, 4, 10, 12, and 18). In the first and second columns, we represented the results for second and third orders of Rayleigh-Schrödinger perturbations, respectively, and in the third column the results for coupled-cluster singles and doubles. In the first row the orbitals by Krieger, Li, and Iafrate were used, versus Hartree-Fock orbitals in the second row.

C. Correlated methods for Ψ

In this section the approximations specific to the wave function part of the coupling are established based on a numerical study. The first approximation is for the method used to describe the fictitious system. The second approximation deals with the definition of the orbital space, referred to as the choice of the reference wave function in last section.

To begin with, let us make an estimation of the errors for the fully interaction system. Three methods will be examined to that goal among the standards of quantum chemistry: second- and third-order Rayleigh-Schrödinger perturbations and coupled clusters with single and double excitations. Furthermore, the influence of the orbitals will be discussed. On that subject, quite remarkably, the results obtained with KS orbitals for the He, Be, and Ne series have been found to be very similar to those obtained with the KLI orbitals. Hence the KS results are not reported in the following. We rather focus on the comparison between KLI and HF orbitals, which is more pronounced. For performing the calculations a numerical program [18] has been used. An overview of the results is reported in Fig. 5. The reader interested in more details, including technical details, is referred to Ref. [19]. In brief, the conclusions for the fully interacting system are the following. First, second-order perturbations prove in great error when used with KLI orbitals [in contrast with the OEP-MBPT(2) scheme proposed by Bartlett *et al.* [20]]. For instance, in the Ar series discrepancies of second-order energies with respect to exact results by Chakravorty *et al.* [21] reach nearly 100 mhartree. Moreover, even with Hartree-Fock orbitals second-order perturbations are wrong by tens of mhartrees in the Be series. Third-order energies rectify those results, but not enough for our present accuracy prerequisite of a few mhartrees, depending on the system inves-

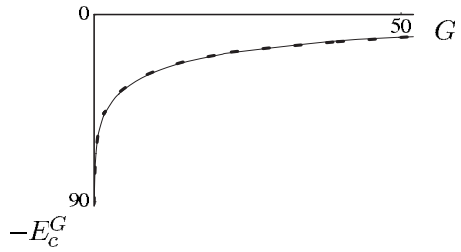

FIG. 6. Correlation energy E_c^G (in mhartree) for the fictitious beryllium atom with gap shift G (in hartree) using KLI orbitals (solid line) and Hartree-Fock orbitals (dashed line).

tigated. Finally, the coupled-cluster method is found to meet our criterium nicely. In addition, it is revealed to be relatively invariant to the choice of orbitals. Accordingly, it will be retained in our subsequent investigations. Of course, this method is expensive, but it is intended for restricted use. It will only be applied to calculate that part of the correlation energy that can be efficiently described with a wave function (as mentioned in Sec. III C). As a further argument, our present purpose is to probe a method where the density-functional part does not allow *a priori* for systematic improvements. Hence is it of prime importance to avoid uncontrolled cancellations of errors in the wave function part of the calculations by making it as exact as possible. Then, of course, in further work addressing more realistic systems the coupled-cluster part of the calculations can be replaced by a more affordable choice.

Once validated for the fully interacting system under study, the coupled-cluster method has been applied to fictitious systems, using either KLI or HF orbitals. Illustrative results are presented for the beryllium atom with gap shift G (Fig. 6) and for the beryllium atom with cutoff κ (Fig. 7), using KLI and HF orbitals. In the gap shift case, (Fig. 6), it is found that whatever G, E_c^G depends very weakly on the choice of orbitals between KLI and HF. Let us recall that these findings simply corroborate previous coupled-cluster results for the fully interacting system. As a rule, from one value of G to another, the orbital space is just left unchanged and, in principle, complete. Only the weights of the determinants in the wave function are modulated according to G, which can be considered as an energetic penalty to the Hamiltonian. Thus, it is not surprising that a rotation in the virtual spectrum does not significantly affect the results. In

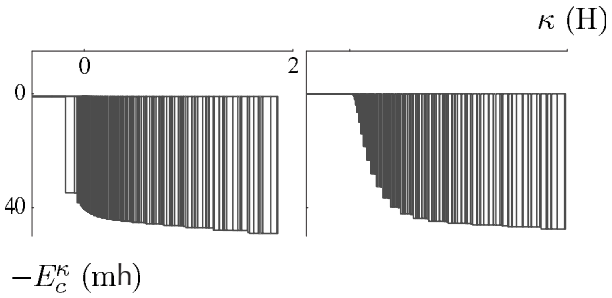

FIG. 7. Correlation energy E_c^κ (in mhartree) for the fictitious beryllium atom with cutoff κ (in hartree) using KLI orbitals (left) and Hartree-Fock orbitals (right).

the cutoff variant the conclusion is just the opposite: a strong dependence on E_c^κ is noted according to the orbitals used, either KLI or HF. This time the reason is that from one finite κ to another the orbital space is not the same and it is no longer complete. Thus, for a given value of κ one cannot go from KLI to HF orbital subspace by a rotation. Under those circumstances the intrinsic nature of each virtual orbital plays a role, which is important especially in the case of near degeneracy. In particular, in the Be atom low-lying virtual orbitals are known to present different spatial distributions and energies, either in the KLI or in the HF scheme. On the one hand, due to the hydrogenic long-range behavior of the KLI potential first virtual KLI orbitals are localized and bound, leading to significant contributions to the correlation energy. On the other hand, low-lying HF virtual orbitals are widely delocalized and energetically close to zero because the HF potential is too repulsive towards them. As a consequence, they contributes very little, individually, to the correlation energy. It is mentioned in passing that this phenomenon is often not observed when standard basis sets are used. This is only due to the fact that basis sets optimized for the correlation energy are contracted in the region of occupied orbitals.

Briefly, for the coupling with gap shift the choice of orbitals is found to be irrelevant at the present level of accuracy (i.e., below 1 mhartree). On the contrary, KLI and HF orbitals produce quite different correlation energies for the system with cutoff κ at small κ. KLI orbitals are eventually retained because they are localized in space as if they had been sort of "optimized" for describing the correlation energy in the small subspace limited by κ. Such a behavior in the wave function part of the coupling is all the more desirable as the density functional in charge of the complement $E_c - E_c^\kappa$ is known to be inadequate for describing near degeneracies (see discussion in Sec. II A). We remind the reader that present developements aim at extracting near degeneracies from the density-functional part of the calculations and defer those effects to a wave function treatment.

D. Approximations for ρ

In this section, the approximations for the density part of the coupling are presented. One common strategy to approximate the universal density functional is to use as a starting point some data calculated in the homogeneous electron gas. Along that line is the local density approximation (LDA), which proved very successful for metallic solids. In that approximation, the correlation energy density per particle of the homogeneous electron gas is simply transferred to the system of chemical interest. As a further step, it has been proposed to account for the inhomogeneity of the density by adding gradient corrections, based on perturbation theory. Those corrections were specially intended for systems having a gap above the Fermi level (in, e.g., semiconductors, atoms, molecules). A review of the various attempts to use gradients in density functionals can be found in Ref. [22]. For the present purpose, we start with the local approximation, and then, in Sec. VI C a gradient correction is introduced in a nonstandard manner. Here we comment on the

first step where the local density approximation has been extended to the fictitious systems of Sec. III A. Let us recall the usual LDA, where at each point in space the correlation energy density of the fully interacting system is replaced by the one of the homogeneous electron gas having the same density. By contrast, presently, at each point of space the correlation energy density of the fictitious system with a gap (cutoff) will be replaced by the one of a homogeneous electron gas with a gap (cutoff) and having the same density. For that purpose the correlation energy of the homogeneous electron gas with a gap (cutoff) has been calculated by applying the coupled-cluster approach of Bishop and Lührmann [23,24]. Technical details are defered to Appendix A (Appendix B) for the definition of these functionals and to the EPAPS materials (Sec. III) [9] for the definition of the cylindrical coordinates that have been used in their evaluation.

There comes the problem to connect the gap in the electron gas with the gap in the atom. As a gap is initially present in the atom but not in the electron gas, the transfer is not obvious from one system to another. In fact, defining the gap in the electron gas is equivalent to finding the universal functional of the density for the coupling. In order to make progress toward a proper definition, several proposals have been tested in the following section, leading to successive improvements for the resulting functionals.

VI. NUMERICAL RESULTS AND REFINEMENT OF THE APPROXIMATIONS

The numerical tests to be performed on the coupling should deal with both its wave function and density parts.

For the wave function part, the starting approximations (discussed in Sec. V C) have already fulfilled our accuracy requirements. Let us remind the reader that the coupled cluster method was eventually chosen as, in contrast with conventional second- and third-order perturbations, it provided acceptable errors for the fully interacting system (0–10 mhartree depending on the system). In conjunction with the coupled cluster method, KLI orbitals were selected as they account for near degeneracies in the fictitious system. Such a property might have been obtained with KS or natural orbitals as well, but for higher computational cost, and HF orbitals are not suited in that respect.

Let us focus on the density-functional part of the coupling for the remaining of the section. As we will see, in that part the starting approximations (shortly described in Sec. V D) do not present a self-contained definition. Instead, they are ambiguously related to the electron gas with a gap (cutoff). Therefore the definition of the gap (cutoff) in the electron gas to be related with the gap (cutoff) in the atom is a matter of choice. In order to gain around the optimal definition of that gap (cutoff) we propose to go through successive numerical experiments. Thus, three definitions for the gap (cutoff) will be considered, and their relative performance will be compared. In Sec. VI A, the simplest choice is presented where the gap (cutoff) in the electron gas is defined with respect to the highest occupied molecular orbital in the atom. In Sec. VI B, we further impose the functional to satisfy an exact derivative property with respect to the coupling parameter.

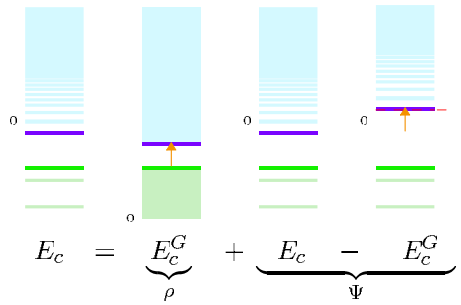

FIG. 8. (Color online) One-particle spectra of the fictitious systems involved in the approximate coupling with gap shift. From left to right: FIS, electron gas with gap shift, FIS, and partially interacting system with gap shift. Ψ (ρ) designates the part of the calculation deferred to the wave function (density) approach.

Toward that goal a global constant is added to the cutoff in the electron gas, which improves significantly the density-functional results for the He and Be series. By contrast the same operation within the gap shift variant has no positive role. Finally, in Sec. VI C a semilocal component is added to the cutoff in the electron gas to better satisfy the same derivative property, providing this time an accurate density functional for all isoelectronic series (He, Be, Ne, Mg, Ar).

A. Same gap (cutoff) for the atom and the electron gas

As mentioned in Sec. V D, the first proposal for defining the gap (cutoff) in the electron gas is to mimic the one in the atom, as shown schematically in Fig. 8 (Fig. 9).

1. Gap-shift and cutoff results in the He and Be series

Figures 9 and 10 display the density part of the coupling (as defined in last subsection) for a range of coupling parameters. We recall that the density part is E_c^G for the gap shift variant (left section of the figures) and $E_c - E_c^\kappa$ for the cutoff variant (right section of the figures). Moreover, these approximate results (bottom curves) have been plotted together with their estimated exact values (top curves) from a wave function calculation based on the KLI and coupled cluster methods (same conditions as in Sec. V C). To ease compari-

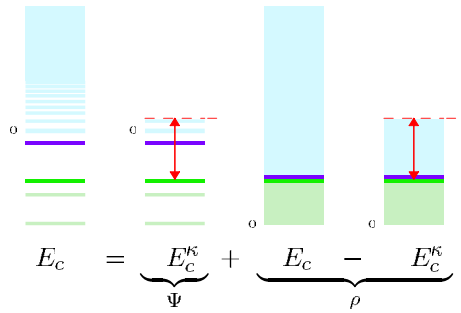

FIG. 9. (Color online) One-particle spectra of the fictitious systems involved in the approximate coupling with cutoff. From left to right: FIS, partially interacting system with cutoff, fully interacting electron gas, and electron gas with cutoff. Ψ (ρ) designates the part of the calculation deferred to the wave function (density) approach.

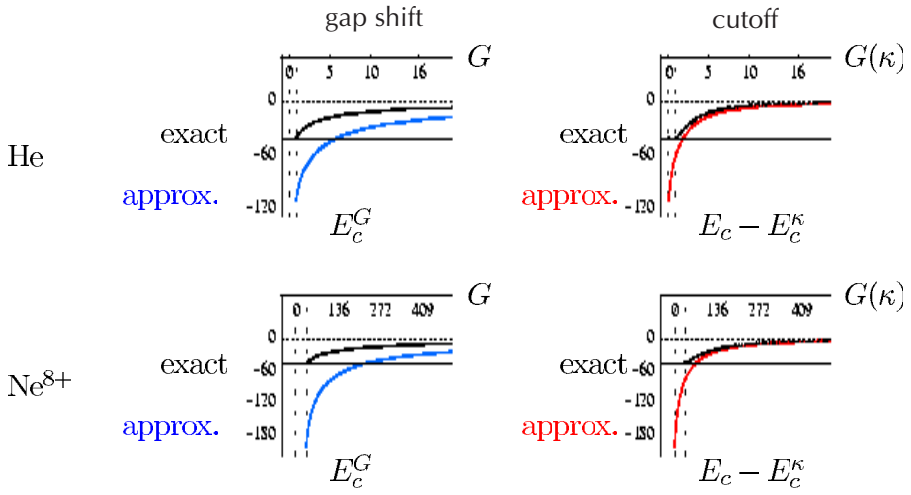

FIG. 10. (Color online) The figure is made of four plots and each plot is made of two curves (above and below). He (first line), Ne^{8+} (second line). Gap shift variant (left), cutoff variant (right). Exact ρ part of the coupling (black, above), approximate ρ part of the coupling (colored, below), in mhartree, depending on G, in hartree. $G(\kappa)$ is related to κ in Eq. (26).

son between the gap shift and cutoff variants in these plots, an arbitrary relationship has been introduced between parameters G and κ,

$$G = \kappa - \epsilon_{homo}. \tag{26}$$

Then, only one of them, G, has been retained to represent the results. Moreover, in the figures dealing with the cutoff variant the notation $G(\kappa)$ has been used in replacement of G to emphasize its dependence on κ [through Eq. (26)]. Figure 10 (Fig. 11) deals with two systems in the He (Be) isoelectronic series. These two systems have been chosen as the neutral atom (top plots) and one of its highly charged cation (bottom plots) in order to see evolution in the series. Intermediate cases display intermediate behaviors and hence are not reported (they are available upon request). In the Be series evolution is expected to be strong due to near degeneracies, in contrast with the He series.

Our results are the following. In all cases, the maximal error occurs when the density functional deals with the fully interacting system—i.e., for the smallest values of the coupling parameters ($G=0$ for the gap shift variant and $\kappa = \epsilon_{homo}$ for the cutoff variant). In those situations the wave function has no contribution to the correlation energy within the coupling and the density-functional part is equivalent to the local density approximation applied to the fully interacting system. Then, as G increases the absolute error of the density functional reduces monotonically. It ultimately vanishes when the noninteracting system is reached by the density functional ($G \to \infty$ for the gap shift variant and $\kappa \to \infty$ for the cutoff variant). In that case, only the wave function contributes to the coupling.

2. Asymptotic considerations of fictitious systems with gap shift and cutoff

Let us further comment on the results obtained previously with the gap shift and the cutoff variants. The noninteracting system is reached significantly faster (i.e., for smaller values of the coupling parameter) with the cutoff variant, compared with the gap shift variant. Moreover, this conclusion stands for the exact results as well as for the approximate ones. In fact, this numerical evidence might have been expected. In the gap shift case, the assymptotic behavior of E_c^G was found to be proportional to G^{-1}, the coefficient being different in the exact and in the approximate cases in general [8]. Similarily, it is shown in the EPAPS material (Sec. IV) [9] that for the cutoff variant the approximate E_c^κ is proportional to $\kappa^{-3} \propto G^{-3/2}$. As a final remark let us recall that for the cutoff variant the exact curve is discontinuous (even if the points are close from each other), whereas it is continuous for the approximate curve.

3. Efficiency of the couplings

Now comes the question of the optimal choice for the coupling parameter, from the point of view of computational efficiency. Let us consider, for the discussion, the beryllium atom in the cutoff variant (Fig. 11, right). We recall that for the reference calculation (top curve) a numerical program was used, including 15 angular symmetries and 200 orbitals per symmetry. Therefore, if the approximate functional (bottom curve) were considered as accurate for $E_c - E_c^\kappa$ after, say, $\kappa=30$ a.u., then hundreds of orbitals would have participated in the complementary wave function part of the calculation, E_c^κ. As a conclusion, the coupling presently defined is quite expensive, even though less expensive than a full wave function calculation. By contrast, in the gap shift variant (Fig. 11, left) with the present computing procedure the cost is just the same for any G, as all orbitals are always included. However, for sufficiently small G numerical error cancellations should occur within the wave function part of the coupling. Indeed in that case a given excitation in the one-particle spectrum has a comparable weight in the correlation energy, dealing either with the fully interacting system or with the fictitious system. Thus the errors should cancel by difference of those two contributions. All things considered, it is concluded that the smaller the coupling parameters (either G or κ), the better the efficiency in the coupling. However, with the present

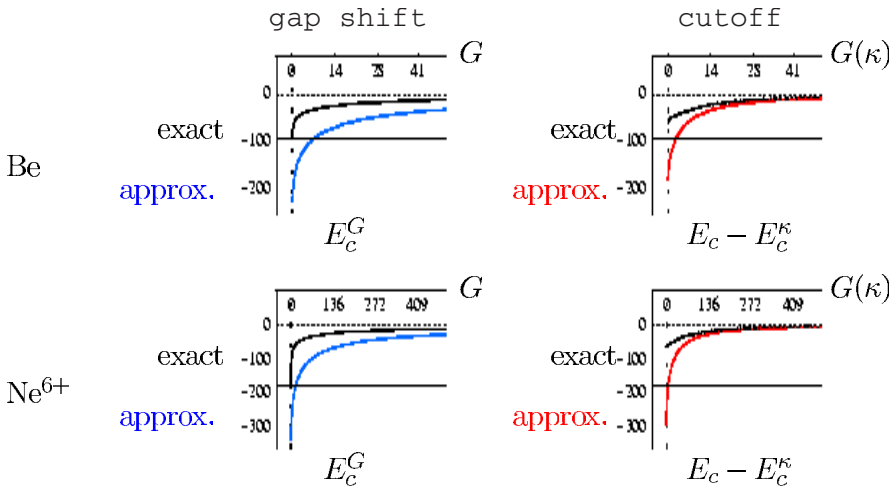

FIG. 11. (Color online) The figure is made of four plots and each plot is made of two curves (above and below). Be (first line), Ne^{6+} (second line). Gap-shift variant (left), cutoff variant (right). Exact ρ part of the coupling (black, above), approximate ρ part of the coupling (colored, below), in mhartree, depending on G, in hartree. $G(\kappa)$ is related to κ in Eq. (26).

definition of the gap (cutoff) in the electron gas, the coupling parameter cannot be chosen small enough for achieving efficiency. Consequently, as a further approximation it will be proposed to associate a given coupling parameter in the atom with a larger parameter in the electron gas. In that way, we expect to make up for the difference in the origin of the one-particle spectrum when the atom is compared with the electron gas. Also, we might compensate for the contribution of the continuous states in the electron gas which are not present in the atom.

B. Gap (cutoff) of the electron gas augmented by a global constant specific to the system

As a first proposal to put this idea into practice, the coupling parameter in the atom, p, will be connected to a larger parameter in the electron gas, $p+t$, t being a global constant of the system. At this stage let us make a remark about the universality the corresponding functional. According to the Hohenberg-Kohn theorem, if our model is correct, the functional is universal and hence should depend only on the density and arbitrary parameter p. Following from that, parameter t is expected to be found ultimately either system independent or as a functional of the density and p. In order to find an adequate parametrization for our model, now, t will be adjusted in order to satisfy an exact relation: the derivative of the density functional with respect to the coupling parameter should be the same in the exact and in the approximate calculations. In other words, the density-functional results will be translated right on the G axis so as to fit their coupled-cluster estimate. Through that procedure we not only expect the exact and approximate derivatives to equate for one given value of G. We also expect agreement for a whole region: the region of large G's. Indeed, for infinite G the density-functional contribution is zero by construction, as it should be. Moreover, at large G this contribution arises by correlating high-lying orbitals, which are reputed to be quite transferable from the electron gas to the atom.

1. Gap-shift and cutoff results in the He and Be series

For the gap shift variant we report our findings in Fig. 12 (He series) and EPAPS (Fig. 1) [9] (Be series). In a given series the two top plots deal with the neutral atom and the two bottom plots with its isoelectronic cation. The two right plots are for the functional without translation, E_c^G, to be compared with the two left plots for the functional with translation, E_c^{G+t}. In each plot the density-functional curve has been superimposed with its coupled-cluster estimate. The translation t used in the left figures are attempts to reproduce the large-G region. As can be seen, neither in the He series nor in the Be series is the global translation a satisfying process. At large G the density-functional curve is very flat and it crosses the coupled-cluster reference whereas at small G it is completely wrong.

The same results are reported for the cutoff variant, in the He series (Fig. 13) and in the Be series (Fig. 14). The two right plots are for the functional without translation, $E_c - E_c^\kappa$, to be compared with the two left plots for the functional with translation, $E_c - E_c^{\kappa+t}$. Contrary to the gap shift variant, and quite remarkably, with the cutoff variant a translation t was found such that the functional reproduced the coupled-cluster results with a good accuracy in the whole range of virtual cutoffs for the He series and for $\kappa > \epsilon_{2p}$ in the Be series. Thus, this time the functional $E_c - E_c^{\kappa+t}$ reveals a good approximation.

a. Origin of the discrepancies between the gap shift and cutoff variants. In order to interpret qualitatively the above results, let us first emphasize an intrinsic difference between the atom and the electron gas due their respective boundary conditions. An atom has an energy gap above the highest occupied orbital, whereas in the electron gas the Fermi level is degenerated with the first virtual levels. This fact has an important consequence on the density-functional part of the coupling. Indeed, the largest discrepancies in that part are known to result from excitations towards the low-lying atomic orbitals. Moreover, in the gap shift variant those low-lying atomic one-particle states are always present, whatever

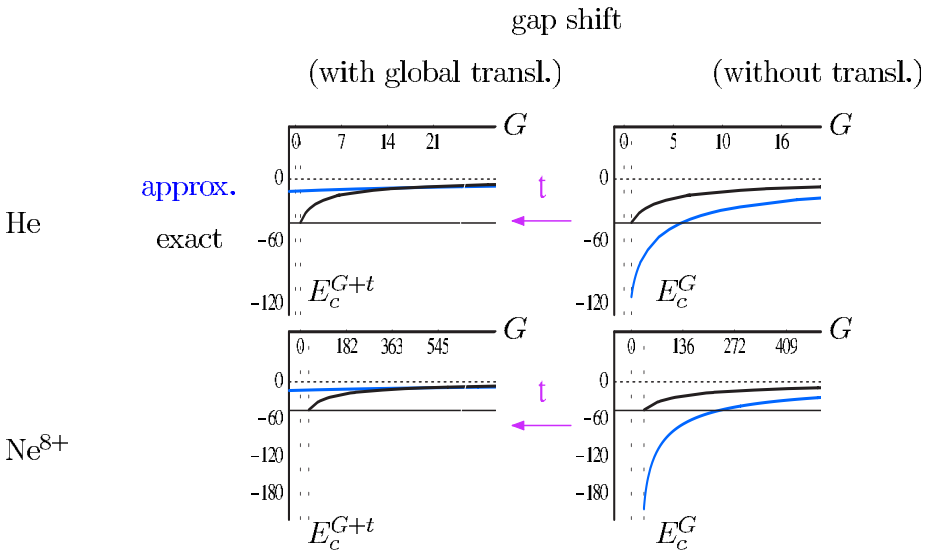

FIG. 12. (Color online) The figure is made of four plots and each plot is made of two curves (above and below). He (first line), Ne^{8+} (second line). Gap shift variant (right), gap shift plus global translation t variant (left). Exact ρ part of the coupling (black, below in the left plots, above in the right plots), approximate ρ part of the coupling (blue, above in the left plots, below in the right plots), in mhartree, depending on G, in hartree. $G(\kappa)$ is related to κ in Eq. (26).

the value of G (see Fig. 8). Only their weight in the correlated wave function is weakened by the gap shift, compared with the fully interacting atom. Therefore, it can be understood that the addition of an increasing gap shift does not correct the functional efficiently, even in the absence of near degeneracies. In the cutoff variant, by contrast, the very system-specific low-lying atomic orbitals are truncated (by the action of a projector) from the density part as soon as $\kappa > \epsilon_{\text{lumo}}$ (see Fig. 9). Thus the non transferable contribution of these low-lying atomic states is then handled by the wave function part, resulting in an improved functional within the coupling. Because of these reasons, it is not surprising that the cutoff variant performs better than the gap shift variant. Accordingly, we propose in the following to focus on the cutoff variant.

b. Efficiency of the coupling with cutoff. From a quantitative point of view much has been gained by introducing the translation t in the cutoff variant. Indeed, we conclude from Fig. 13 that the wave function part of the coupling can simply be avoided by performing such a translation in the He series. If the cutoff is given its smallest value—i.e., just above the highest occupied orbital ($\kappa = \epsilon_{2s}$)—the whole correlation energy of the fully interacting system is obtained only from the electron gas with a cutoff $\epsilon_\kappa + t$, t being a global constant. For the Be series, the balance is hardly more expensive. In that case the minimal value of κ allowing a good approximation for the density-functional part of the coupling is such that $\epsilon_\kappa = \epsilon_{lumo} = \epsilon_{2p}$. Then, the wave function part of the coupling is reduced to the virtual active space containing near-degenerate $2p$ orbitals, which are bounded since the KLI potential has been used to generate the orbital space. In brief, we have found that the density functional with cutoff plus global translation has an appropriate form to model the contribution of high-lying orbitals to the correlation energy, in whole (for the He series) or at least in part (for the Be series).

From a practical point of view, now, the translation t which is specific to the system has to be determined. This can be achieved rigorously, for instance, by implementing a least-squares procedure between the exact and approximate functional derivatives in the range where that mapping is obtained ($\kappa \geqslant \epsilon_{2s}$ in the He series and $\kappa > \epsilon_{2p}$ in the Be series,

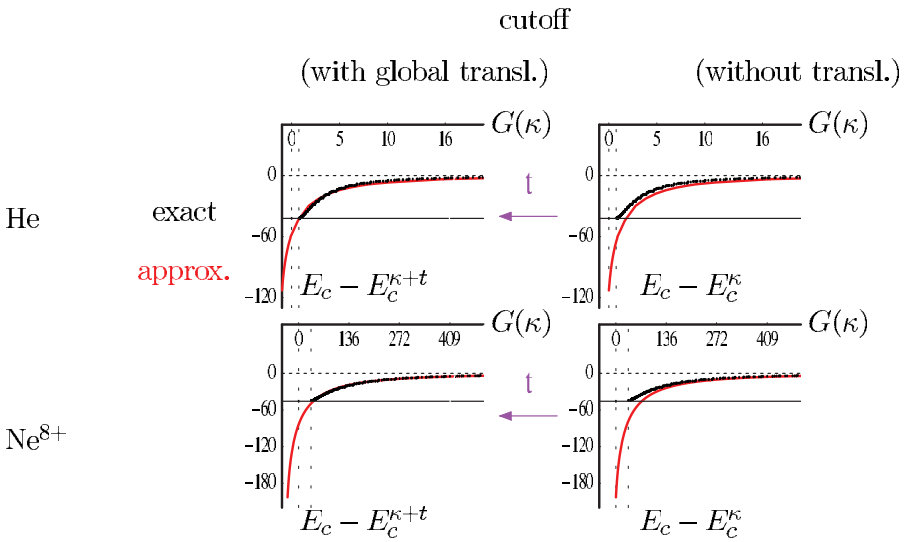

FIG. 13. (Color online) The figure is made of four plots and each plot is made of two curves (above and below). He (first line), Ne^{8+} (second line). Cutoff variant (right), cutoff plus global translation t variant (left). Exact ρ part of the coupling (black, above in the right plots, superimposed in the left plots), approximate ρ part of the coupling (red, below in the right plots, superimposed in the left plots), in mhartree, depending on G, in hartree. $G(\kappa)$ is related to κ in Eq. (26).

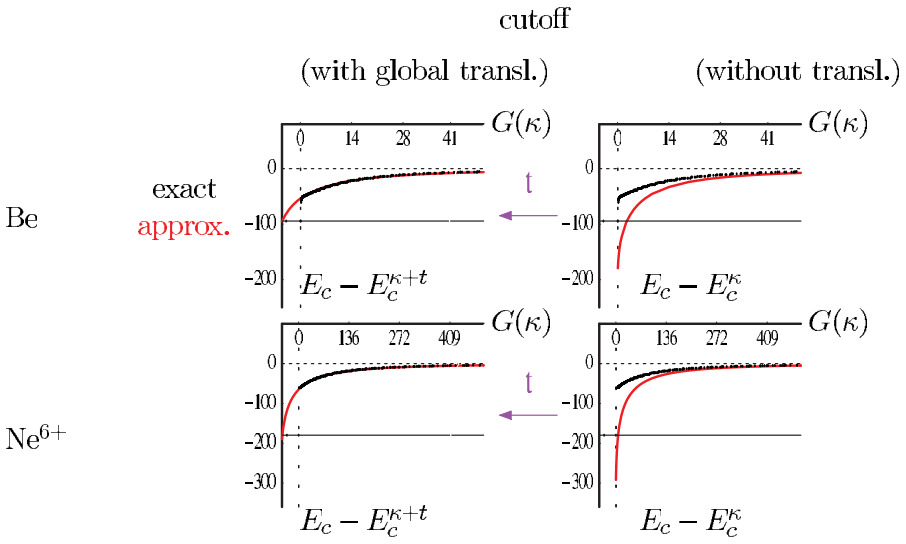

FIG. 14. (Color online) The figure is made of four plots and each plot is made of two curves (above and below). Be (first line), Ne^{6+} (second line). Cutoff variant (right), cutoff plus global translation t variant (left). Exact ρ part of the coupling (black, above in the right plots, superimposed in the left plots), approximate ρ part of the coupling (red, below in the right plots, superimposed in the left plots), in mhartree, depending on G, in hartree. $G(\kappa)$ is related to κ in Eq. (26).

as seen before). Let us mention that for such a mathematical procedure it is convenient that the functional with cutoff is made continuous. That can be obtained by replacing, in Eq. (7), the θ step function by a smooth function with the same limit behaviors. At this stage we propose a more efficient recipe to find the translation t, from a computational point of view. For calculating a derivative, only two points are required. Therefore we suggest to calculate only two (or a few) points in the coupled-cluster curve, which are located in the range allowed for the mapping ($\kappa \geqslant \epsilon_{2s}$ in the He series and $\kappa > \epsilon_{2p}$ in the Be series) and which are not too expensive. In brief we recommend small values of κ contained in the range allowed for the mapping. In that way the cost of the procedure remains very advantageous compared with a full wave function calculation. As another advantage, small values of κ automatically belong to the part of the curve where the slope is the largest. Thus, from such points the most reliable numerical values of the translation t can be extracted.

2. Cutoff results in the Ne, Mg, and Ar series

Let us see what happens now in more complicated systems such as the Ne, Mg, and Ar series. The results are plotted in Fig. 15 for the Ne series. In that case, by contrast with the results previously obtained for the He and Be series, no translation t could be found to make the resulting approximate functional valid in the whole range of virtual κ's. Alternatively, several such translations seem to be required according to the domain of κ under consideration. Mainly two such domains can be distinguished: the region of small κ's, where E_c^κ is decreasing quickly with κ, and the region of large κ's, where E_c^κ is decreasing slowly with κ. This result suggests that each shell in the atom should be treated separately. The same conclusions arise for the Mg and Ar series, and therefore the corresponding figures are not repeated. Following from this, in the next section it will be proposed that the atom with cutoff κ be associated with an electron gas with a cutoff varying in space in a semilocal way. The expression for the cutoff will be taken as $\frac{1}{8}|\frac{\nabla\rho}{\rho}|^2+t$, and the motivations for that choice are explained in the next section.

C. Cutoff of the electron gas augmented by the semilocal quantity $\frac{1}{8}|\frac{\nabla\rho}{\rho}|^2$ plus a global constant t

In the standard approach based on wave functions, correlation is produced by interacting Slater determinants. Moreover, those interactions are efficient if the orbitals involved overlap themselves and are close in energy. According to that criterium, frontier orbitals are of prime importance provided they are sufficiently localized such as KLI or KS orbitals. However, whenever a core orbital comes into play LUMO is not necessarily its best partner for contributing to the correlation energy. One can wonder now about an equivalent proximity criterium within the present density-functional approach. In other words, is it possible to extract from the electron gas a one-particule spectral region that should be put into interaction so as to account for the correlation energy in the atom with cutoff? Atomic orbitals and plane waves being different objects, we will only test the transferability of energy gaps between the atom and the electron gas in that purpose. As an obvious attempt, one might think of taking the energy gap from atomic frontier orbitals and puting it into the electron gas above the Fermi level. However, as previously mentioned, transferring the atomic HOMO-LUMO gap in the electron gas is not expected to be optimal in cases where core orbitals do correlate with virtual orbitals in the atom. Thus we conclude that the cutoff needs be defined locally in the electron gas to take into account the spatial distribution of the correlating orbitals in the atom according to its shell structure. In each region of space the gap should thus correspond to the pair of occupied and virtual orbitals that contribute most to the correlation energy. We illustrate our proposal in the Be atom. In that case, according to what was just proposed above the cutoff in the electron gas should reproduce the $2s$-$2p$ gap in the valence region and the $1s$-$2p$ gap in the inner region. As a generalization, it will be proposed in the following to take the gap in the electron gas as the ionization potential of the shell (up to a global constant t, possibly different from the one of last section) in each point of the coordinate space. Moreover, as a first estimation of this local ionisation potential the semilocal expression $\frac{1}{8}|\frac{\nabla\rho}{\rho}|^2$ was retained [25–27]. In order to motivate

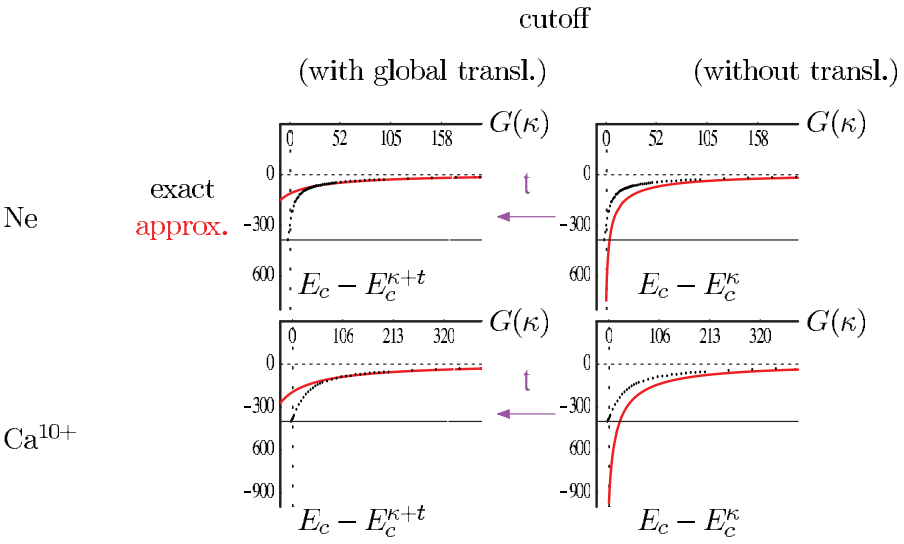

FIG. 15. (Color online) The figure is made of four plots and each plot is made of two curves (above and below). Ne (first line), Ca^{10+} (second line). Cutoff variant (right), cutoff plus global translation t variant (left). Exact ρ part of the coupling (black, above in the right plots, below in the left plots), approximate ρ part of the coupling (red, below in the right plots, above in the left plots), in mhartree, depending on G, in hartree. $G(\kappa)$ is related to κ in Eq. (26).

that choice, the latter function has been plotted for some elements of the He and Be series, to be found in the EPAPS material (Figs. 2 and 3) [9]. Moreover, those plots have been compared with the radial density of the systems considered. In the He series, it is concluded that the function $\frac{1}{8}|\frac{\nabla\rho}{\rho}|^2$ is in fact roughly a constant in space and close to the ionization potential of the first shell (IP_{1s}). By contrast, in the Be series, the same function varies between the ionization potentials of the first and second shells (IP_{1s} and IP_{2s}, respectively), in accordance with their spatial distribution.

1. Results in the He and Be series

In this section the accuracy of the density functional based on an electron gas with cutoff $\frac{1}{8}|\frac{\nabla\rho}{\rho}|^2+t$ just defined is put to the test for the He and Be series (cf. Figs. 16 and 17, respectively). Moreover, the results are compared with the ones previously obtained from an electron gas with a constant cutoff (Figs. 13 and 14, respectively). As a conclusion the results are found to be practically unchanged for the following reasons. In the He series, let us recall that the quantity $\frac{1}{8}|\frac{\nabla\rho}{\rho}|^2$ was nearly a global constant in space, numerically close to the ionization potential of orbital $1s$ (see discussion just above Sec. VI C 1). Therefore it is not surprising that once the global translation t has been properly adjusted, again the coupling is found to be valid in the whole range of virtual κ's and no wave function contribution is required. By contrast, $\frac{1}{8}|\frac{\nabla\rho}{\rho}|^2$ was not a constant in the Be series; as discussed just above Sec. VI C 1, it varied between the ionization potentials of the core and valence shells. However, again the results of the coupling are unchanged (cf. Fig. 17): after some global translation the functional proves to be sufficiently accurate in the range $\kappa > \epsilon_{2p}$, so that only the contribution of orbital $2p$ needs be deferred to the wave function part of the calculation. In that case, the reason why the results are unchanged is simply that the range of small κ's affected by the local variations of the cutoff is less than the global constant required for the translation t. As a consequence, the change for the approximate functional (from Fig. 14 to Fig. 17) is observed only beyond its domain of applicability—that is to say, in the region reserved for the wave function part of the coupling.

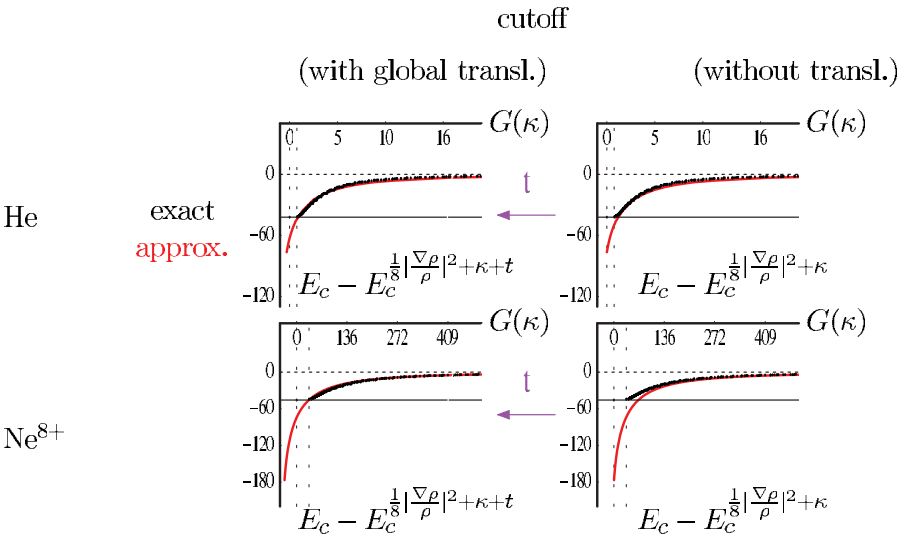

FIG. 16. (Color online) The figure is made of four plots and each plot is made of two curves (above and below). He (first line), Ne^{8+} (second line). Local cutoff $\frac{1}{8}|\frac{\nabla\rho}{\rho}|^2$ variant (right), local cutoff plus global translation t variant (left). Exact ρ part of the coupling (black, above or superimposed), approximate ρ part of the coupling (red, below or superimposed), in mhartree, depending on G, in hartree. $G(\kappa)$ is related to κ in Eq. (26).

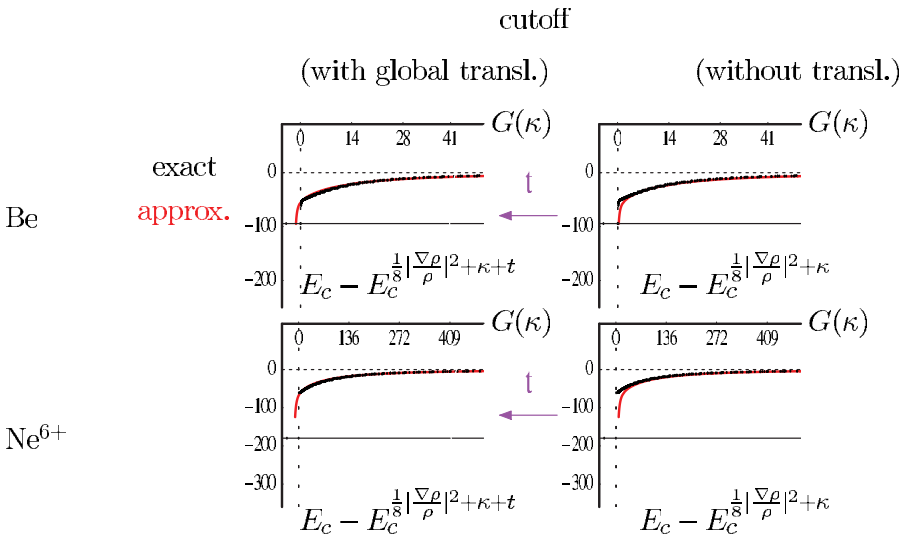

FIG. 17. (Color online) The figure is made of four plots and each plot is made of two curves (above and below). Be (first line), Ne^{6+} (second line). Local cutoff $\frac{1}{8}|\frac{\nabla\rho}{\rho}|^2$ variant (right), local cutoff plus global translation t variant (left). Exact ρ part of the coupling (black, above or superimposed), approximate ρ part of the coupling (red, below or superimposed), in mhartree, depending on G, in hartree. $G(\kappa)$ is related to κ in Eq. (26).

2. Results in the Ne, Mg, and Ar series

In brief, the coupling with cutoff revealed to be quite efficient in the He and Be series, whether the local change of the cutoff in the electron gas was taken into account (Sec. VI C 1) or not (Sec. VI B 1). By contrast, in the Ne, Mg, and Ar series it was concluded that the variant with a constant cutoff in the electron gas could not be used (cf. Sec. VI C 2) because its local dependence on the shell structure was crucial in the range of small κ's. In order to correct this last feature the semilocal cutoff $\frac{1}{8}|\frac{\nabla\rho}{\rho}|^2$ was proposed and the corresponding results are reported in Fig. 18 for the Ne series and in the EPAPS material (Figs. 4 and 5) [9] for the Mg and Ar series. Indeed, these results show that the coupling with cutoff can be corrected by the electron gas with a semilocal cutoff defined as $\frac{1}{8}|\frac{\nabla\rho}{\rho}|^2$. In the Ne series, where no near degeneracies are present, the situation is found to be quite similar to that of the He series: the functional is valid for all virtual κ, so that the wave function part of the coupling can simply be avoided. Such is also the case for the magnesium atom, the argon atom, and its first cations. By contrast, for the higher charged cations in the Mg and Ar series near degeneracies occur because the orbital ordering of the hydrogenoid ions is gradually recovered as nuclear charges increase. However, in those cases like in the Be series, the coupling with semilocal cutoff can be used in a very efficient way provided the near-degenerate states are included in the wave function part of the calculation. Finally, it might be added that in the Mg and Ar series, near-degenerate states yield a significantly lower proportion of the correlation energy than in the Be series. Thus, by exclusion of the Be series the present semilocal density functional is already quite accurate to account for the correlation energy in the first closed-shell atoms and their isoelectronic series.

3. Translation values for the functional with local cutoff

Translations t used in combination with the coupling with local cutoff (in Secs. VI C 1 and VI C 2) are given in Fig. 19. These values have been plotted for all systems against their ionization potential by Chakravorty *et al.* [21]. As can be seen, the translations are very small for neutral atoms and they increase with ionization potential (and nuclear charge) in a series in a nearly linear way. Interestingly, in complete

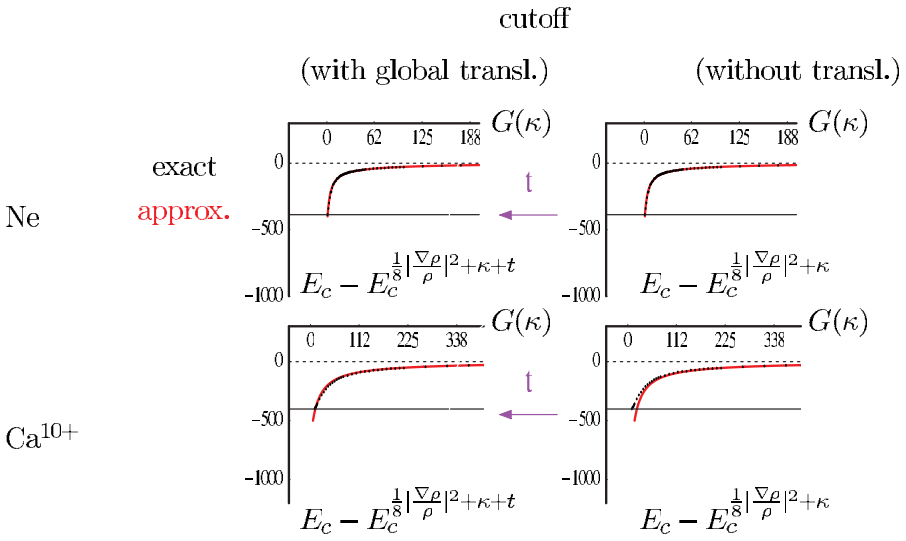

FIG. 18. (Color online) The figure is made of four plots and each plot is made of two curves (above and below). Ne (first line), Ca^{10+} (second line). Local cutoff variant $\frac{1}{8}|\frac{\nabla\rho}{\rho}|^2$ (right), local cutoff plus global translation t variant (left). Exact ρ part of the coupling (black, above or superimposed), approximate ρ part of the coupling (red, below or superimposed), in mhartree, depending on G, in hartree. $G(\kappa)$ is related to κ in Eq. (26).

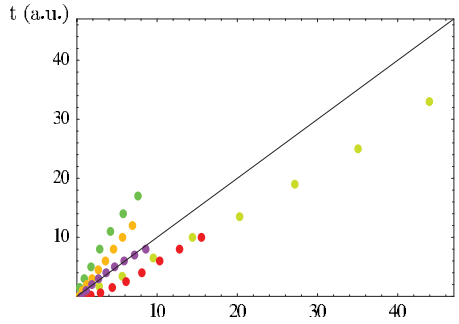

FIG. 19. (Color online) Global translations (t in hartree) for the functional $E_c - E_c^{(|\nabla\rho/\rho|^2+\kappa+t)/8}$ versus ionization potentials (IP in hartree). In order of increasing slope: Ne series (red, IP$<$20), He series (yellow, IP$<$50), Ar series (violet), Mg series (orange), and Be series (green).

shells which are not quasidegenerated (He and Ne series), the slopes are very close to each other and lower than 1. By contrast, in incomplete shells which are quasidegenerated (Be, Mg, Ar series) the slopes are greater than (or close to) 1 and they differ significantly depending on the series: the more pronounced the degeneracy, the larger the slope.

VII. CONCLUSIONS AND PROSPECTS

Among all the methods used in quantum chemistry for describing the ground-state energy, some of those resolving the Schrödinger equation are appropriate for rendering the correlation effects due to near degeneracies. Moreover, other methods grounded on density-functional theory are often suitable in the absence of near degeneracies. From these observations it was proposed that wave function and density functionals be combined, so that the entire correlation effects are depicted properly. In the couplings presently examined the configurational space for the wave function has been divided into two fractions. Then, each fraction has been attributed to a different method. The special feature of the present couplings, compared with the usual density functionals, is that exact results can be approached in a systematic way from the structure of the orbital space. Once the formalism had been built for these couplings, some approximations have been defined and refinements have been gained as the numerical experiments proceeded. The atoms He, Be, Ne, Mg, and Ar and their first isoelectronic cations were used as a benchmark in these calculations for the following reasons: on the one hand, these systems are simple enough to be handled by the most accurate methods; on the other hand, they are sufficiently complex for possibly displaying near degeneracies. It turned out that the present couplings lead to quite encouraging results when the wave function contribution arises from a coupled-cluster formalism restricted to a small orbital space and the density functional contribution is extracted from an electron gas with cutoff such that the local variations of the atomic ionisation potential are reproduced. In future work, this last variant will be applied to molecules. An important point to achieve for this extension will be to test the effect of using standard Gaussian basis sets for a method based on the proper description of the orbital space. Then, from a physical point of view, it will be of great interest to see whether the present coupling is able to manage other situations which are known as critical for standard density functionals such as hydrogen bonds, van der Waals interactions, covalent bond breakings and spin degeneracies, charge transfer, etc.

ACKNOWLEDGMENTS

The authors would like to thank S. Salomonson and P. Öster for providing their atomic numerical coupled-cluster code [18] and J.-L. Heully for explaining its content. As a result, the authors were able to adapt this code to the present couplings between wave function and density functionals. J. B. Krieger is warmly acknowledged for reading the manuscript. He also participated in stimulating discussions around the KLI potential [17] and the Krieger-Chen-Iafrate-Savin density functional [27], which influenced the present choice of semilocal gap. Finally, the Centre de Calculs Recherche et Enseignement (CCRE, University P. and M. Curie — Jussieu, France) is acknowledged for generous allocation of computer time.

APPENDIX A: APPROXIMATION rpa*+rpaex*(1) FOR THE ELECTRON GAS WITH GAP SHIFT G

The correlation energy of an electron gas with gap shift has already been calculated by Rey and Savin [8] using as a starting point the coupled-cluster method proposed by Freeman for an electron gas [28]. Towards that goal, they noticed that the projector operator for the system with gap shift $\hat{O}^G$ was a one-particle operator, like the kinetic operator. Therefore, in the original equations of Freeman the kinetic energy contribution of the virtual orbitals was simply incremented by G. In the present work, the same kind of calculations were performed by adapting the RPA*+RPAEX*(1) method by Bishop and Lührman for an electron gas [24]. The method by Bishop and Lührmann was chosen because it was found to be slightly more stable than the method by Freeman from a numerical point of view and even simpler to implement [29]. Indeed, in the former analytical integrals could be used to a larger extent, due to an additional approximation where the contributions of the occupied momenta were averaged. In other respects, in both cases the agreement with the Monte Carlo results by Ceperley and Alder [30] was better than 1 mhartree in the domain of atomic densities. In this Appendix, note that all momenta $(\mathbf{k},\mathbf{k}_1,\mathbf{k}_2)$ have been put in adimentional units by dividing them by the norm of the Fermi momentum. Moreover, the energy gap G has been put in adimentional units by dividing it by the squared norm of the Fermi momentum. The correlation energy for the electron gas with gap shift G, $\epsilon_c^G(r_s)$, is expressed as

$$\epsilon_c^G(r_s) = \epsilon_c^{\mathrm{RPA}^\star,G}(r_s) + \epsilon_c^{\mathrm{RPAEX}^\star(1),G}(r_s), \tag{A1}$$

with

$$\epsilon_c^{\mathrm{RPA}^\star,G}(r_s) = \left[\frac{1}{\alpha r_s}\right]\left[\frac{2}{\pi}\right]\int_0^\infty dq\, \bar{S}_2^{\mathrm{R},G}(r_s,q)$$

$$\epsilon_c^{\mathrm{RPAEX}^\star(1),G}(r_s) = -\frac{1}{2}\left[\frac{1}{\alpha r_s}\right]\left[\frac{2}{\pi}\right]\int_0^\infty dq \frac{\langle q_{ex}^{-2}e^{-1}\rangle^G}{\langle e^{-1}\rangle^G}\bar{S}_2^{\mathrm{R},G}(r_s,q), \tag{A2}$$

$\bar{S}_2^{\mathrm{R},G}(r_s,q)$ being the solution of the second-order equation which remained bounded at large momenta q:

$$\bar{S}_2^{\mathrm{R},G}(r_s,q) = -(\alpha r_s)\left[\frac{4}{3\pi}\right]\frac{1}{q^2}\langle e^{-1}\rangle^G P^2(q)\left[1+\frac{\bar{S}_2^{\mathrm{R},G}(r_s,q)}{P(q)}\right]^2. \tag{A3}$$

In the above formula the following definitions were used:

$$P(q) = \frac{3}{4\pi}\int d\mathbf{k}\,\theta(\mathbf{k}_1,\mathbf{q}), \tag{A4}$$

$$\langle e^{-1}\rangle^G = \left[\frac{3}{4\pi P(q)}\right]^2\int d\mathbf{k}_1 d\mathbf{k}_2\left[\frac{1}{e+2G}\right]\theta(\mathbf{k}_1,\mathbf{q})\,\theta(-\mathbf{k}_2,\mathbf{q}), \tag{A5}$$

$$\langle q_{ex}^{-2}e^{-1}\rangle^G = \left[\frac{3}{4\pi P(q)}\right]^2\int d\mathbf{k}_1 d\mathbf{k}_2\left[\frac{1}{q_{ex}^2(e+2G)}\right]\theta(\mathbf{k}_1,\mathbf{q})\,\theta(-\mathbf{k}_2,\mathbf{q}), \tag{A6}$$

In formulas (A4)–(A6), θ is the step function defined by $\theta(\mathbf{k},\mathbf{q})=\theta(1-\mathrm{k})\,\theta(|\mathbf{k}+\mathbf{q}|-1)$ and $\theta(x)=1$ if $x\geqslant 0,0$ otherwise. The kinetic contribution e was defined as the scalar product $e=\mathbf{q}(\mathbf{k}_2-\mathbf{k}_1-\mathbf{q})$. The constant α is defined as $\alpha=[4/(9\pi)]^{1/3}$.

APPENDIX B: APPROXIMATION rpa*+rpaex*(1) FOR THE ELECTRON GAS WITH CUTOFF κ

For the electron gas with cutoff, the equations of Bishop and Lührmann have been modified such that all integrals over virtual momenta $\mathbf{k}$ are restricted to the range $k<\kappa$. For that purpose, step functions have been used. In this appendix, note that all momenta $(\mathbf{k},\mathbf{k}_1,\mathbf{k}_2,\kappa)$ have been put in adimensional units by dividing them by the norm of the Fermi momentum. The correlation energy of the electron gas with cutoff κ is expressed as

$$\epsilon_c^\kappa(r_s) = \epsilon_c^{\mathrm{RPA}^\star,\kappa}(r_s) + \epsilon_c^{\mathrm{RPAEX}^\star(1),\kappa}(r_s), \tag{B1}$$

with

$$\epsilon_c^{\mathrm{RPA}^\star,\kappa}(r_s) = \left[\frac{1}{\alpha r_s}\right]\left[\frac{2}{\pi}\right]\int_0^\infty dq\,\bar{S}_2^{\mathrm{R},\kappa}(r_s,q),$$

$$\epsilon_c^{\mathrm{RPAEX}^\star(1),\kappa}(r_s) = -\frac{1}{2}\left[\frac{1}{\alpha r_s}\right]\left[\frac{2}{\pi}\right]\int_0^\infty dq \frac{\langle q_{ex}^{-2}e^{-1}\rangle^\kappa}{\langle e^{-1}\rangle^\kappa}\bar{S}_2^{\mathrm{R},\kappa}(r_s,q). \tag{B2}$$

In Eqs. (B2), $\bar{S}_2^{\mathrm{R},\kappa}(r_s,q)$ corresponds to the solution of the following second-order equation, which remains bounded at large momenta,

$$\bar{S}_2^{\mathrm{R},\kappa}(r_s,q) = -(\alpha r_s)\left[\frac{4}{3\pi}\right]\frac{1}{q^2}\langle e^{-1}\rangle^\kappa P^{\kappa 2}(q)\left[1+\frac{\bar{S}_2^{\mathrm{R},\kappa}(r_s,q)}{P^\kappa(q)}\right]^2, \tag{B3}$$

and the following integrals have been used:

$$P^\kappa(q) = \frac{3}{4\pi}\int d\mathbf{k}\,\theta^\kappa(\mathbf{k}_1,\mathbf{q}), \tag{B4}$$

with $\theta^\kappa(\mathbf{k},\mathbf{q})=\theta(1-\mathrm{k})\,\theta(|\mathbf{k}+\mathbf{q}|-1)\,\theta(\kappa-|\mathbf{k}+\mathbf{q}|)$,

$$\langle e^{-1}\rangle^\kappa = \left[\frac{3}{4\pi P^\kappa(q)}\right]^2\int d\mathbf{k}_1 d\mathbf{k}_2\left[\frac{1}{e}\right]\theta^\kappa(\mathbf{k}_1,\mathbf{q})\,\theta^\kappa(-\mathbf{k}_2,\mathbf{q}) \tag{B5}$$

and

$$\langle q_{ex}^{-2}e^{-1}\rangle^\kappa = \left[\frac{3}{4\pi P^\kappa(q)}\right]^2\int d\mathbf{k}_1 d\mathbf{k}_2\left[\frac{1}{q_{ex}^2 e}\right]\times\theta^\kappa(\mathbf{k}_1,\mathbf{q})\times\theta^\kappa(-\mathbf{k}_2,\mathbf{q}). \tag{B6}$$

[1] T. Helgaker, P. Jørgensen, and J. Olsen, *Molecular Electronic-Structure Theory* (Wiley, New York, 2002).
[2] T. Helgaker, T. Ruden, P. Jørgensen, J. Olsen, and W. Klopper, J. Phys. Org. Chem. **17**, 913 (2004).
[3] L. H. Thomas, Proc. Cambridge Philos. Soc. **23**, 542 (1927).
[4] E. Fermi, Rend. Accad. Naz. Lincei **6**, 602 (1928).
[5] W. Kohn and L. J. Sham, Phys. Rev. **140**, A1133 (1965).
[6] P. Hohenberg and W. Kohn, Phys. Rev. **136**, B864 (1964).
[7] A. Savin, in *Density Functional Methods in Chemistry*, edited by J. K. Labanowski and J. W. Andzelm (Springer-Verlag, Berlin, 1991).
[8] J. Rey and A. Savin, Int. J. Quantum Chem. **69**, 581 (1998).
[9] See EPAPS Document No. E-PLRAAN-75-119702 for Sec. I, present approach related to the Kohn-Sham methods; Sec. II, arbitrariness in the definition of the correlation energy; Sec. III, cylindrical coordinates for evaluating the integrals; Sec. IV, asymptotic behavior of the density functional for the fictitious system with cutoff κ at large κ; Fig. 1, gap shift variant in the Be series; Fig. 2, semilocal gap and radial density in the He series; Fig. 3, semilocal gap and radial density in the Be series; Fig. 4, cutoff variant with the semilocal gap in the Mg series; Fig. 5, cutoff variant with the semilocal gap in the Ar series. For more information on EPAPS, see http://www.aip.org/pubservs/epaps.html.
[10] M. Levy, Proc. Natl. Acad. Sci. U.S.A. **76**, 6062 (1979).
[11] E. R. Davidson, Int. J. Quantum Chem. **69**, 241 (1998).
[12] A. A. Jarzecki and E. R. Davidson, Phys. Rev. A **58**, 1902 (1998).
[13] V. N. Staroverov, G. E. Scuseria, J. P. Perdew, J. Tao, and E. R. Davidson, Phys. Rev. A **70**, 012502 (2004).

[14] H. Stoll, E. Golka, and H. Preuss, Theor. Chim. Acta **55**, 28 (1980).
[15] A. Savin, H. Stoll, and H. Preuss, Theor. Chim. Acta **70**, 407 (1986).
[16] E. K. U. Gross, M. Petersilka, and T. Grabo, in *Chemical Applications of Density Functional Theory*, edited by B. B. Laird, R. B. Ross, and T. Ziegler (Oxford University Press, Oxford, 1996).
[17] J. B. Krieger, Y. Li, and G. J. Iafrate, *Recent Developments in Kohn-Sham Theory for Orbital-dependant Exchange-correlation Energy Functionals* (Plenum Press, New York, 1995).
[18] S. Salomonson, I. Lindgren, and A. M. Martenson, Phys. Scr. **21**, 351 (1980).
[19] C. Gutlé, J. L. Heully, J. B. Krieger, and A. Savin, Phys. Rev. A **66**, 012504 (2002).
[20] R. J. Bartlett, I. Grabowski, S. Hirata, and S. Ivanov, J. Chem. Phys. **122**, 034104 (2005).
[21] S. J. Chakravorty, S. R. Gwaltney, E. R. Davidson, F. A. Parpia, and C. F. Fischer, Phys. Rev. A **47**, 3649 (1993).
[22] U. von Barth, Phys. Scr. **T109**, 9 (2004).
[23] R. F. Bishop and K. H. Lührmann, Phys. Rev. B **17**, 3757 (1978).
[24] R. F. Bishop and K. H. Lührmann, Phys. Rev. B **26**, 5523 (1982).
[25] J. P. Perdew, R. G. Parr, M. Levy, and J. L. Balduz, Phys. Rev. Lett. **49**, 1691 (1982).
[26] M. Kohout, A. Savin, and H. Preuss, J. Chem. Phys. **95**, 1928 (1991).
[27] J. B. Krieger, J. Chen, J. Iafrate, and A. Savin, *Electron Correlations and Material Properties: Construction of an Accurate Self-Interaction-Corrected Correlation Energy Functional Based on an Electron Gas with a Gap* (Plenum, New York, 1999).
[28] D. L. Freeman, Phys. Rev. B **15**, 5512 (1977).
[29] F. Merzel, Ph. D. thesis, University of Ljubljana, 1998.
[30] D. M. Ceperley and B. J. Alder, Phys. Rev. Lett. **45**, 566 (1980).
[31] J. E. Harriman, Phys. Rev. A **27**, 632 (1983).